CSIRO PUBLISHING

www.publish.csiro.au/journals/ijwf *International Journal of Wildland Fire* **2009**, *18*, 865–874

Flame interactions and burning characteristics of two live leaf samples[1]

Brent M. Pickett[A], *Carl Isackson*[A], *Rebecca Wunder*[A], *Thomas H. Fletcher*[A,D], *Bret W. Butler*[B] *and David R. Weise*[C]

[A]Department of Chemical Engineering, Brigham Young University, Provo, UT 84602, USA.
[B]USDA Forest Service, Rocky Mountain Research Station, Fire Sciences Laboratory, Missoula, MT 59808, USA.
[C]USDA Forest Service, Pacific Southwest Research Station, Forest Fire Laboratory, Riverside, CA 92507, USA.
[D]Corresponding author. Email: tom_fletcher@byu.edu

Abstract. Combustion experiments were performed over a flat-flame burner that provided the heat source for multiple leaf samples. Interactions of the combustion behavior between two leaf samples were studied. Two leaves were placed in the path of the flat-flame burner, with the top leaf 2.5 cm above the bottom leaf. Local gas and particle temperatures, as well as local oxygen concentrations, were measured along with burning characteristics of both leaves. Results showed that the time to ignition of the upper leaf was not significantly affected by the presence of the lower leaf. The major difference observed was that the time of flame duration of the upper leaf was significantly affected by the presence of the lower leaf. Causes for the prolonged flame were found to be the consumption of oxygen by the burning lower leaf and the obstruction provided by the lower leaf, causing a wake effect, thus altering the combustion behavior of the upper leaf.

Introduction

Wildland fires burn through large areas of live vegetation throughout the world. The ability to predict the spread of these wildland fires is paramount in protecting both property and ecology. Particularly in North America, operational wildland fire spread models (models used by fire managers in the field) are based primarily on empirical correlations developed from 'dead' fuels such as excelsior or cast pine needles (Byram 1959; Fosberg and Deeming 1971; Rothermel 1972; Van Wagner 1973; Albini 1976; Forestry Canada Fire Danger Group 1992). However, fires do not spread exclusively through dead fuels, but rather through a combination of dead and 'live' fuels. Operational field models (Deeming *et al*. 1972; Andrews 1986; Forestry Canada Fire Danger Group 1992; Coleman and Sullivan 1996; Finney 1998) based on these dead fuel correlations can help fire managers better determine how fast a fire will move through a known area of fuel type, slope and wind speed (spread rate). These operational models predict fire spread rate well for the conditions for which the model was correlated (e.g. dead fuels), but they do not perform as well for live fuels (Catchpole *et al*. 2002).

Limited research has been performed on live, individual leaf samples. Dimitrakopoulos and Papaioannou (2001) used an ISO standards test method (ISO 5657–1986E) to determine the flammability of 24 Mediterranean plant species. Weise *et al*. (2005) determined seasonal differences and flammability of various ornamental vegetation using a cone calorimeter (ASTM E 1354); they also reviewed live forest fuel combustion over the last 30 years. Both of these techniques used radiant furnaces to supply the heat source to the foliage sample. Smith (2005), Fletcher *et al*. (2007), and Pickett (2008) have studied combustion characteristics of live, individual samples by using a convective heat source (flat-flame burner) that simulates an oncoming fire front. These investigators determined both qualitative and quantitative differences for 14 species found throughout the United States (California, intermountain west, and south-east regions). Generally, fire spread is determined by the rate of ignition of individual foliage samples. The ignited foliage subsequently burns and ignites nearby foliage samples. Combustion studies have been performed on stationary wood particles in wind tunnels to study brand formation (e.g. Tarifa *et al*. 1965 and Pagni and Woycheese 2000) and furnaces (e.g. Lu 2006), but none, to the authors' knowledge, have incorporated multiple samples.

This study will focus on the interactions between two leaf samples, including evaporation, combustion, and heating rates. Using this more fundamental approach (two-leaf system) rather than a fuel bed will give more insight on how these interactions influence the overall combustion behavior, particularly in ignition and flame propagation through a bush. With a knowledge of the fundamental combustion interactions (particularly fluid dynamics and oxygen concentrations) gained from this study, wildland fire prediction through modeling can be improved at all

[1]Part of this manuscript was prepared by US Government employees on official time and with government funding and is therefore in the public domain and not subject to copyright in the US.

10.1071/WF08143 1049-8001/09/070865

scales (individual leaf models to full-scale atmospheric models). Future work will be to focus on the scale-up of some of these modeling efforts in going from an individual leaf model to a multi-leaf model.

Experimental materials

Three plant species were selected from western regions of the United States and used for the experimental analysis: hoaryleaf ceanothus (*Ceanothus crassifolius*)[2], Eastwood's manzanita (*Arctostaphylos glandulosa*), and gambel oak (*Quercus gambelii* Nutt.). Ceanothus and manzanita samples were harvested at the North Mountain Experimental Area adjacent to the San Bernardino National Forest in California and were selected because of their uniformity in dimensions (i.e. closest disc-like shape). Samples were sealed and sent overnight to Brigham Young University (BYU) for testing. Gambel oak samples were harvested in forest areas surrounding Provo, Utah, and were selected because of their ease of collection. Experiments on live samples were performed within 2 days of arrival to BYU to ensure freshness (i.e. to retain original moisture).

Experimental apparatus

The original experimental apparatus was designed to simulate a wildland fire approaching an individual fuel sample, mimicking temperatures and heating rates in wildland fires, which are thought to be ~1200 K (Butler *et al*. 2004*b*) and 100 K s^{-1} (Butler *et al*. 2004*a*) respectively. To simulate these wildland fire conditions, the fuel sample was attached by an alligator clip to a stationary horizontal rod positioned on a mass balance (see Fig. 1). A counter-weight stabilized the rod and fuel sample. A flat-flame burner (FFB) was placed on a moveable platform that provided a convective heat source to the fuel sample. The burner flame was 1–3 mm high, with post-flame conditions of 987 ± 12°C ($\pm$ indicates the standard deviation) and 10 mol% O_2 at 5 cm above the FFB. Heat fluxes for this apparatus configuration were reported to be 80–140 kW m^{-2} (Fletcher *et al*. 2007). Individual samples experimented on this apparatus number over 2000. Further details of the apparatus and procedure are described in detail by Engstrom *et al*. (2004), Fletcher *et al*. (2007), and Pickett (2008).

The original apparatus (described above) was altered to incorporate multiple leaf samples. No changes were made to the FFB, only the location of leaves or equipment. Leaf samples and other equipment were placed at one of two positions directly above the FFB: position A at 4.0 cm or position B at 6.5 cm; using these distances, an IR camera could see both surfaces of the leaves at an angle of ~45°. Various configurations were designed to isolate differences in variables (e.g. t_{ig} – time to ignition, T_{ig} – ignition temperature) at both positions. Three types of equipment were used in the flame: (i) a thermocouple (Omega type-K (chromel–alumel), 127-μm bead diameter) to measure the gas temperature (T_{gas}) at the desired position; (ii) an O_2 analyzer that measured the local O_2 concentration (mol %) at a distance between positions A and B (~5.3 cm above the FFB); and (iii) a non-combustible metal disc used to replace a leaf at position A in order to compare the effects of fluid dynamics on ignition. Leaves at position B were placed on a mass balance, while temperatures for both leaves were obtained with an IR camera. A summary of the different configurations are found both in Fig. 2 and in Table 1. The definition of each configuration will be used extensively in this paper; thus both schematic and tabular forms are displayed.

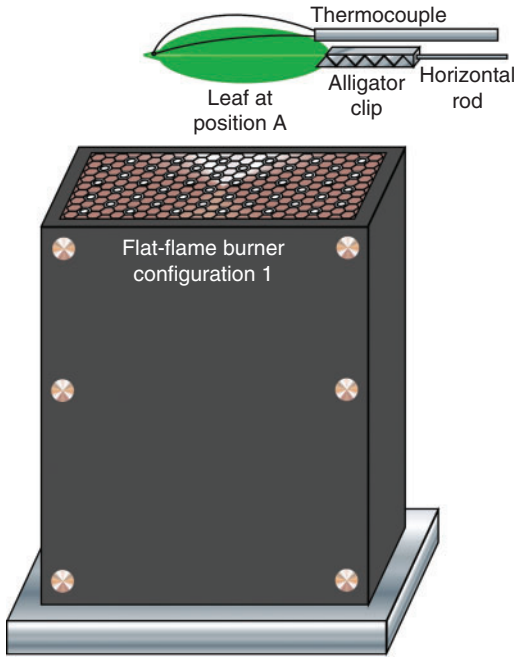

Fig. 1. Schematic of a single-leaf at position A with embedded thermocouple (original apparatus – configuration 1).

The thermocouple in configurations 2–4 measured T_{gas} at position B, not the leaf temperature. As only one mass balance was programmed for data collection, the mass history for the two-leaf configurations (i.e. configurations 2 and 6) was recorded only on leaf samples at position B. From the mass history of leaf B, mass release rates were determined and analyzed. Similarly sized pairs of leaves for each species were selected so as to minimize the effects of mass and surface area. These leaves were selected at random locations from various branches of different plants. Approximately 10 runs (actual number of runs shown in Table 2) were performed for each configuration (e.g. 10 runs for configuration 2 *v.* 10 runs for configuration 3) for each day of experiments. Time constraints as well as equipment failure (e.g. broken thermocouple) inhibited the acquisition of exactly 10 runs for each configuration. Days of experimental sets with corresponding symbols, configurations, and moisture content are shown in Table 2.

Results and discussion

A total of 550 experimental runs were performed on the three species indicated, scattered among the different configurations (Table 2). Time-dependent mass and temperature data were obtained at either location (A or B). The quantities determined

[2]Source for common and scientific plant names – USDA plants database: http://plants.usda.gov, accessed 29 September 2009.

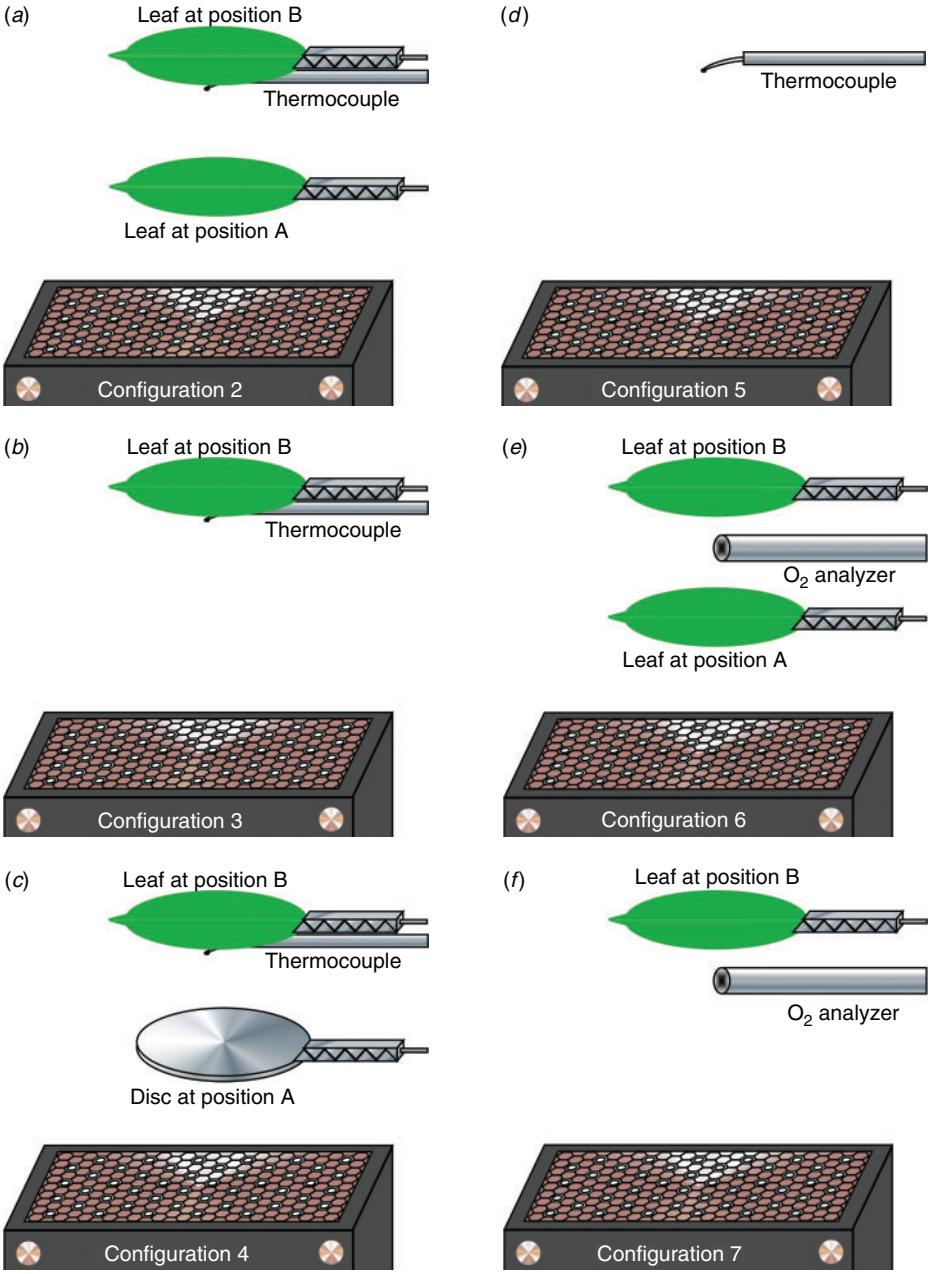

Fig. 2. Schematic of various experimental configurations of leaf samples and equipment at positions A and B and in between. Configuration 2 (*a*); configuration 3 (*b*); configuration 4 (*c*); configuration 5 (*d*); configuration 6 (*e*); and configuration 7 (*f*). Further details for each configuration are found in Table 1.

from each experiment are listed in Table 3. Average values of time and temperature quantities for various configurations are given in Table 4.

Comparison of configurations 2 and 3

The rate of fire spread is thought to be dependent on the ignition of fine fuels (i.e. samples with high surface-to-volume ratio). Ignition times for leaves at positions A and B (t_{ig}^{A}, t_{ig}^{B}) for configuration 2 (leaf/leaf), and t_{ig}^{B} for configuration 3 (no leaf/leaf) were determined. Fig. 3 shows a comparison of t_{ig}^{B} for the two configurations. Confidence intervals (95%) were determined using a standard *t*-test. The t_{ig}^{B} data for a given species in either configuration were the same, as shown in Fig. 3. The only significantly different experimental set of configurations was for dry gambel oak (Gd1) with a moisture content of 8% (dry-weight basis). For this particular set of experiments, t_{ig}^{B} for configuration 2 had 42% higher values than for configuration 3. This means that for the Gd1 experiment, ignition of leaf B was delayed when leaf A was present. This ignition delay of leaf B may have been caused

Table 1. Leaf and equipment positions for the various experimental configurations used with the flat-flame burner
Positions A and B are identified in Fig. 2

Configuration	Position A	Between A and B	Position B
1	Leaf with embedded thermocouple	–	–
2	Leaf	–	Thermocouple (T_{gas}), leaf
3	–	–	Thermocouple (T_{gas}), leaf
4	Metal disc	–	Thermocouple (T_{gas}), leaf
5	–	–	Thermocouple (T_{gas})
6	Leaf	O_2 analyzer	Leaf
7	–	O_2 analyzer	Leaf

Table 2. Matrix of experiments
Moisture content, wt%, dry-weight basis

Species	Symbol	Moisture content (%)	Date	Configurations (no. of runs)
Ceanothus	C1	56.8	1 June 2007	2 (10), 3 (10)
Manzanita	M1	53.3	1 June 2007	2 (10), 3 (5)
Manzanita	M2	42.4	20 June 2007	2 (10), 3 (10)
Manzanita	M3	38.4	8 August 2007	2 (10), 3 (8)
Manzanita	M4	22.7	24 October 2007	2 (10), 3 (10), 4 (10)
Gambel oak	G1	92.0	8 June 2007	2 (10), 3 (10)
Gambel oak	G2	84.1	2 July 2007	2 (10), 3 (10)
Gambel oak	G3	86.1	9 July 2007	2 (10), 3 (10)
Gambel oak	G4	88.2	25 July 2007	2 (10), 3 (10)
Gambel oak	G5	83.4	30 July 2007	2 (10), 3 (10)
Gambel oak	Gd1	7.9	12 July 2007	2 (7), 3 (7)
Gambel oak	Go1	~80	3 July 2007	6 (8), 7 (4)
Gambel oak	Go2	~80	27 July 2007	6 (10), 7 (5)

by the lack of leaf moisture content, because all experimental sets with live fuels (and hence higher moisture contents) did not exhibit similar behavior. However, this may have also been due to the amount of O_2 available to leaf B (discussed below), some O_2 being consumed by leaf A because of its relatively quick ignition. The ignition times for the Gd1 experiment were quite small in both cases, but well within the resolution of the video camera (18–19 Hz). The flow dynamics would be nearly the same for both dead (Gd1) and live fuels (all other experimental sets in Fig. 3), and hence should not cause a difference in t_{ig}^B between dead and live fuels.

The largest difference between configurations 2 and 3 was observed in the flame duration of leaf B (t_{fd}^B), as shown by the data in Fig. 4. Many experiments had significantly different values of t_{fd}^B for configuration 2 compared with configuration 3, always showing a higher t_{fd}^B for configuration 2, indicating that leaf B burned longer with leaf A present. It should be noted that if the confidence intervals were relaxed slightly (perhaps to a 90% confidence interval), even more experimental sets would be statistically different (i.e. manzanita species). Possible causes for this difference in t_{fd}^B may be that the obstruction (leaf A) alters the flow dynamics, or that the combustion of leaf A alters the local amount of O_2 available to leaf B, or a combination of these two phenomena. These two phenomena will be discussed later in this paper.

Another possibly significant variable that can be determined is the ignition delay time (t_{id}) between the leaf at position A and the leaf and position B (defined as $t_{ig}^B - t_{ig}^A$). This was only applicable to configuration 2. Fig. 5 shows the values of t_{ig} of leaves at positions A and B. Values of t_{ig}^B are significantly higher than t_{ig}^A for all gambel oak runs and nearly significant (again assuming relaxed confidence intervals) for some of the manzanita runs. This ignition delay may be due to the size of leaf A, which alters the downstream conditions for leaf B. This would explain why no ignition delay was observed for the ceanothus experiments, because ceanothus leaves are smaller than manzanita or gambel oak leaves.

Most other measured variables proved not to be significantly different at either ignition or burnout between configurations 2 and 3, such as normalized mass, surface temperature from the IR camera, or mass release rate. However, the gas temperature (measured by the thermocouple) and normalized mass were significantly different at other times during the experiment (i.e. other than at ignition or burnout), particularly before ignition. This will be discussed in the following section.

Comparison with configuration 4

To better determine how the presence of leaf A altered the flow dynamics for leaf B, a thin metal disc instead of a leaf was placed at position A (i.e. configuration 4 as seen in Fig. 2*c*). Data from

Table 3. List of measured quantities in the two-leaf configuration experiments

Measured quantity	Definition	Experimental method
Time to ignition (t_{ig})	Difference in time from start of particle heating until first visible flame on or near the leaf surface (either leaf A or B)	Frame-by-frame inspection of video images for presence of sustained, initial flame
Ignition temperature (T_{ig})	Particle temperature at which first visible flame is observed on or near the leaf surface (either leaf A or B)	IR camera, time-synched with the video and focussed on the appropriate leaf tip
Gas temperature (T_{gas})	Gas temperature	Thermocouple, corrected for radiation
Flame duration (t_{fd})	Time difference between burnout (flame extinction) and ignition	Frame-by-frame inspection of video for presence of flame
Ignition delay time (t_{id})	Time difference between the ignitions of leaves B and A	Frame-by-frame inspection of video for presence of flame

this configuration were compared with data from configurations 2 and 3. Rather than just focussing on ignition and burnout, the entire gas temperature (T_{gas}) and normalized mass (m/m_0) histories were averaged and plotted (along with 95% confidence intervals), as shown in Fig. 6 for manzanita samples. The average times for ignition and burnout are displayed with a diamond symbol for each configuration, and the confidence intervals for the times of ignition and burnout are displayed as individual data points (appears to be a thicker line).

The temperature plot (Fig. 6*a*) shows that local gas temperatures in the initial time region (before ignition, 0–1 s) are significantly higher in configuration 3 (no leaf–leaf) than in configurations 2 (leaf–leaf) and 4 (disc–leaf). This behavior was observed for all sets, except for dried gambel oak (Gd1) with a moisture content of 8%. Moisture acted as a heat sink, which yielded lower temperatures initially. The gas temperature at position B (with no leaf present at either position) normally has a profile as shown in configuration 5 (i.e. direct convective gases from the FFB). A constant gas temperature of ~950°C was observed after the initial heat-up region. A dip in the gas temperature occurred in configuration 3 after initially approaching the maximum temperature (~950°C). Leaf B in configuration 3 influenced the temperature recorded by the thermocouple directly beneath it. This dip in temperature was likely caused by moisture or volatiles leaving leaf B, which was not observed in other configurations owing to the obstruction of leaf A for configuration 2 and the metal disc for configuration 4.

The gas temperature underneath leaf B in configuration 4 leveled out at ~500°C, which is significantly lower than configurations 2 and 3 near burnout. The other configurations eventually reached the maximum temperature ~950°C, although not necessarily at the same rate. This lower temperature and lower heating rate observed initially for configuration 4 would prolong the overall combustion process (rate), which was quantifiably observed (see confidence intervals in time for configuration 4 in Fig. 6). Owing to the obstruction from the metal disc, the laminar gases (Reynolds number ≈ 340 around disc-shaped leaf) from the FFB transitioned to turbulent; vortices were created from the edge of the disc and while gases impinged on the upper leaf, causing recirculation of the flow. This was observed qualitatively as the flame from leaf B moved downward to the surface of the metal disc (see Fig. 7). This turbulence could entrain some surrounding air (at room temperature), which cools the gases to the observed temperature of 500°C. Other possible reasons for this lower gas temperature would be radiation from the metal disc (causing heat loss from the disc's surface), and a lack of the combustion process (upstream event) that occurs in configuration 2 but not in configuration 4, particularly when the flame height of leaf A is at a maximum. This observed turbulence did not increase the rate of combustion as would be expected. The prolonged flame duration may instead be due to a wake effect (displacement of heat and gases necessary for combustion) of the obstruction. If the leaf at position B were placed at a longer distance from the obstruction, the wake effect might not be quite as significant. The flow dynamics (particularly the wake effect) were altered by both the leaf at position A (configuration 2) and the metal disc (configuration 3). However, leaf A moved up and down as well as disintegrated owing to combustion, which allowed leaf B to experience less wake

Table 4. Average time and temperature data from various experimental sets of the two-leaf configurations
The second number indicates the ±95% confidence interval. Symbols are: *t*, time; *T*, temperature; *ig*, ignition; *id*, ignition delay; *fd*, flame duration; and *gas*, convective gas. Sets and configurations are defined in Table 1

Set	Configuration	t_{ig} (s)		t_{id} (s)	t_{fd} (s)		T_{ig} (°C)		T_{gas} (°C)
		A	B		A	B	A	B	B
C1	2	6.21 ± 1.36	6.26 ± 0.74	0.05 ± 1.53	10.1 ± 1.59	13.62 ± 1.08	319 ± 50	293 ± 48	NA
	3	–	6.35 ± 1.31	–	–	9.85 ± 1.64	–	269 ± 36	NA
M1	2	2.97 ± 0.83	6.23 ± 2.52	3.26 ± 2.55	14.43 ± 1.65	16.83 ± 4.72	307 ± 46	352 ± 80	NA
	3	–	4.72 ± 2.26	–	–	12.04 ± 4.06	–	245 ± 65	NA
M2	2	2.71 ± 1.23	4.13 ± 0.75	1.42 ± 1.31	12.73 ± 2.03	14.4 ± 1.89	252 ± 42	314 ± 55	372 ± 52
	3	–	2.97 ± 2.48	–	–	10.76 ± 2.14	–	242 ± 94	433 ± 52
M3	2	1.38 ± 0.24	1.59 ± 0.43	0.21 ± 0.51	12 ± 0.49	13.12 ± 1.82	248 ± 28	279 ± 20	704 ± 72
	3	–	1.46 ± 0.26	–	–	10.84 ± 0.7	–	241 ± 32	776 ± 114
M4	2	3.36 ± 1.17	3.49 ± 0.49	0.12 ± 0.96	9.84 ± 1.3	17.36 ± 1.91	362 ± 45	349 ± 85	549 ± 137
	3	–	3.53 ± 1.62	–	–	15.05 ± 1.83	–	256 ± 54	761 ± 132
	4	–	2.69 ± 1.44	–	–	22.97 ± 3.43	–	294 ± 99	522 ± 124
G1	2	0.75 ± 0.17	1.31 ± 0.25	0.56 ± 0.28	6.48 ± 0.76	7.74 ± 0.54	215 ± 30	250 ± 40	422 ± 198
	3	–	1.13 ± 0.26	–	–	5.74 ± 0.36	–	239 ± 35	498 ± 39
G2	2	0.58 ± 0.11	1.07 ± 0.31	0.49 ± 0.39	6.98 ± 0.45	8.02 ± 0.94	286 ± 52	384 ± 105	NA
	3	–	1.15 ± 0.32	–	–	6.27 ± 0.62	–	267 ± 52	NA
G3	2	0.58 ± 0.16	1.17 ± 0.27	0.59 ± 0.26	5.23 ± 0.92	5.87 ± 0.97	278 ± 73	269 ± 114	NA
	3	–	1.03 ± 0.5	–	–	5.54 ± 0.68	–	258 ± 23	NA
G4	2	0.91 ± 0.13	1.51 ± 0.36	0.6 ± 0.37	5.84 ± 0.37	7.91 ± 0.77	308 ± 41	224 ± 34	NA
	3	–	1.26 ± 0.17	–	–	5.11 ± 0.69	–	212 ± 22	NA
G5	2	0.53 ± 0.19	0.95 ± 0.21	0.42 ± 0.25	5.46 ± 0.34	6.97 ± 1.03	237 ± 32	225 ± 29	411 ± 161
	3	–	0.94 ± 0.12	–	–	4.96 ± 0.36	–	244 ± 27	578 ± 159
Gd1	2	0.19 ± 0.05	0.7 ± 0.21	0.51 ± 0.19	3.69 ± 0.9	4.22 ± 0.95	NA	NA	194 ± 106
	3	–	0.41 ± 0.04	–	–	3.11 ± 0.33	–	NA	192 ± 94

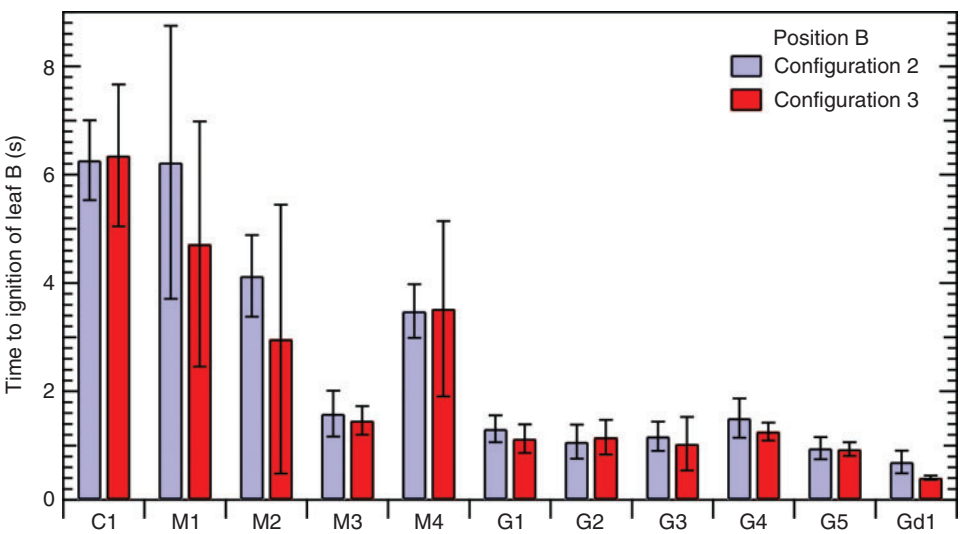

Fig. 3. Comparison of the time to ignition of leaf B (t_{ig}^{B}) for configurations 2 and 3 (leaf–leaf *v.* no leaf–leaf). The 95% confidence intervals are also shown.

effect through the experimental run than with the metal disc at position A.

Fig. 6*b* shows how the normalized mass changes during the experimental run for configurations 2, 3, and 4. The same mass history was observed at early times for configurations 2 and 4 (configurations with obstructions), with significantly lower mass values at the same times in configuration 3. The difference in mass between configuration 3 and the other two configurations is most observable at ignition and 2–3 s following ignition. After this early time period, mass values from configuration 2 (leaf–leaf) started decreasing more rapidly than in configuration 4 (disc–leaf), and started to behave similarly to configuration 3

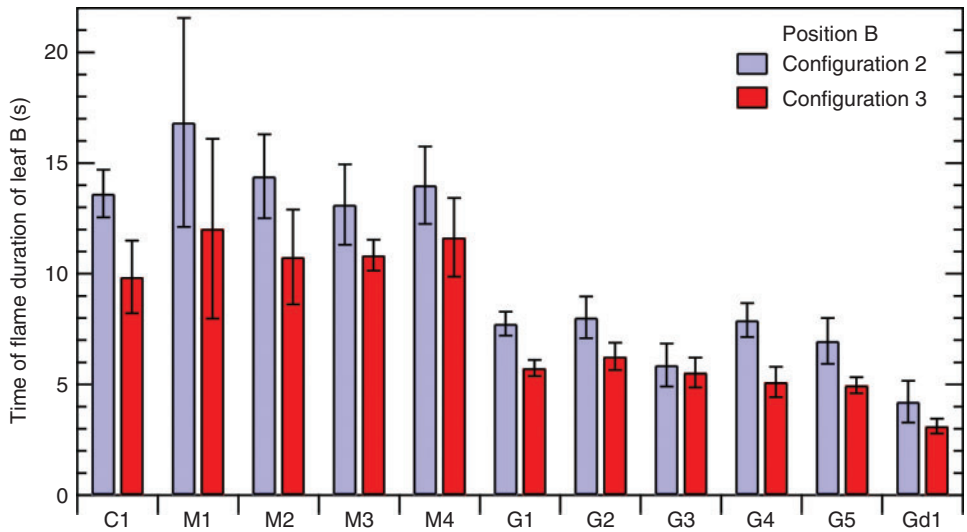

Fig. 4. Comparison of flame duration of leaf B for configurations 2 and 3 (leaf–leaf *v.* no leaf–leaf). The 95% confidence intervals are also shown.

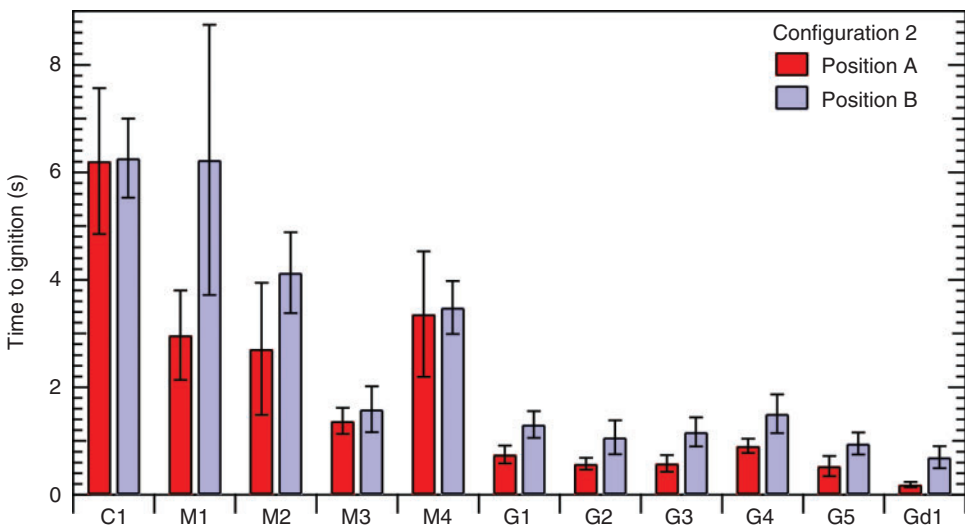

Fig. 5. Comparison of time to ignition values for leaves A and B for configuration 2 (leaf–leaf) with 95% confidence intervals.

(no obstruction). A final value of the normalized mass of ~0.2 was observed in all configurations. As the ash content was ~5 wt% (Fletcher *et al*. 2007) on a dry basis, this means that ~15% of the dry mass did not burn. This ~20% remaining mass is the remaining char and ash left after devolatilization and is consistent with the ASTM proximate analysis reported by Fletcher *et al*. Leaf samples in configuration 3 took longer to burn, which is consistent with the lower gas temperature for this configuration.

From the data in Fig. 6, it can be seen that a leaf at position A does affect the combustion of leaf B, particularly around pre-ignition and ignition. This difference early in the experiment can be attributed to the change in flow dynamics. O_2 is not needed for evaporation and initial pyrolysis, and hence local O_2 concentration should not affect the overall combustion behavior of leaf B early during the experiment (neglecting radiation). The obstructions (configurations 2 and 4) used in these experiments cause a wake effect that displaces heat required to burn leaf B, eventually prolonging the combustion process (i.e. a longer flame duration results).

Comparison of configurations 6 and 7

The O_2 concentration (mol%) of the gas stream was measured at a position between A and B, with the position shown in Fig. 2*e* and Fig. 2*f*. O_2 analyzer measurements were recorded as the minimum value during the experimental run; the analyzer had

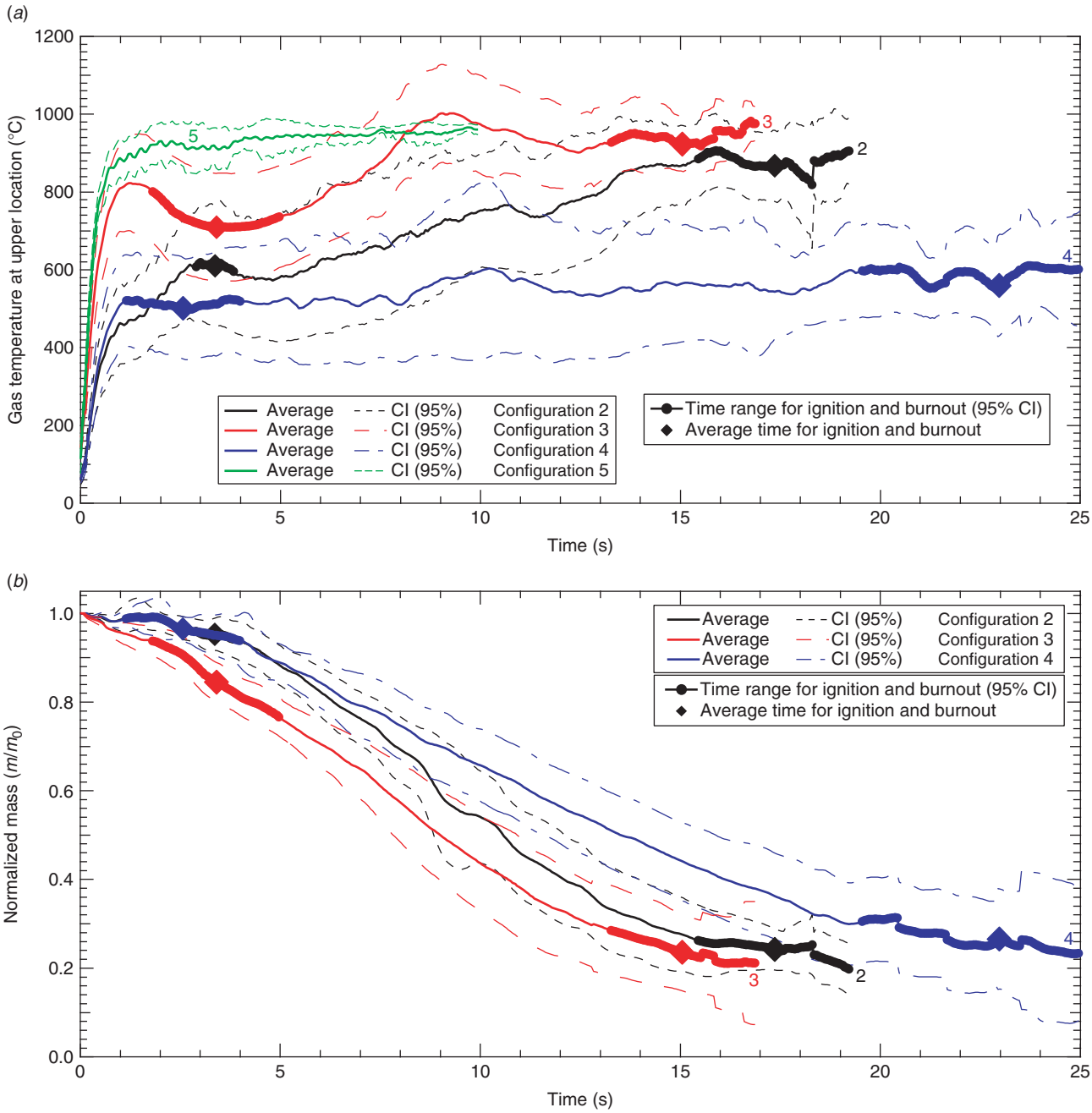

Fig. 6. Gas temperature (from thermocouple) at position B with 95% confidence intervals (configurations 2–5) (*a*). Normalized mass of leaf B with 95% confidence intervals (configurations 2–4) (*b*). These experiments sets were performed with manzanita samples (M4).

a delay of 3–4 s after ignition before a minimum value was obtained, which unfortunately was comparable with the burning times. O_2 data from configurations 6 (leaf–O_2–leaf) and 7 (no leaf–O_2–leaf) are compared in Fig. 8.

The O_2 content is lower (~20%) for the configuration with leaf A present (configuration 6) than with no leaf at position A (configuration 7). It should first be noted that the difference in O_2 between the two configurations for the Go1 experiment is only significant at the 85% confidence interval. The leaf at position A consumes O_2, which limits the amount of O_2 available to leaf B. This may also prolong the flame duration of leaf B, particularly after ignition occurs on leaf A.

These interactions between samples, such as the wake effects and the O_2 consumption, can dramatically affect combustion behavior, and are significant issues for future model development and design. These effects may not be easy to approximate by simply adding single-leaf results together. More studies must be performed to quantitatively determine interactions between samples, along with methods of incorporating the interactions into a wildland fire model.

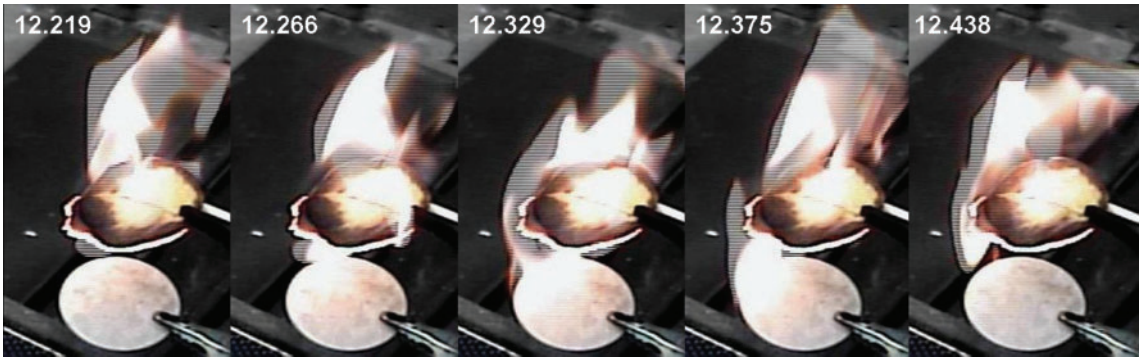

Fig. 7. Sequence showing flame from leaf B moving downward to the surface of the metal disc. Numbers indicate the time difference (s) from the initial time of the experimental run.

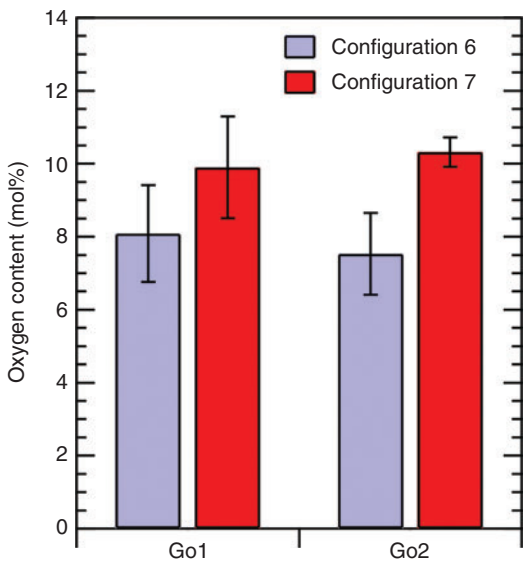

Fig. 8. Comparison of the average value of O_2 content (mol%) in configurations 6 and 7 (leaf–O_2–leaf *v.* no leaf–O_2–leaf) along with 95% confidence intervals.

Conclusions

Combustion experiments were performed using a FFB that ignited two individual forest-fuel samples spaced 2.5 cm apart. Three common forest fuels involved in wildland fires in the western USA were used. Many variations of configurations were analyzed to determine the effects of one leaf on the other. Results show the following significant characteristics when leaf A is present (compared with when there is no leaf at position A):

(1) Longer flame duration of leaf B – prolonged combustion
(2) Lower gas temperature initially (i.e. before ignition and during ignition) at position B
(3) Lower O_2 content at an intermediate position between positions A and B – leaf A consumes a significant amount of O_2.

A significant ignition delay (difference in time of ignitions between two leaves) was observed for larger species (manzanita and gambel oak).

The change of flow dynamics seemed to be important to the combustion process in the two-leaf configuration. Obstructions caused a wake effect and altered both temperature and mass throughout the experiment, particularly in the early stages of the experiment (pre-ignition and ignition). Flow dynamics (particularly wake effects) and the consumption of O_2 of leaf A are two important interactions that affect the combustion behavior in this two-leaf experimental setup. These interactions between leaf samples could have significant implications for future model development from single-leaf results alone.

Acknowledgements

This research was funded by the USDA/USDI National Fire Plan administered through a Research Joint Venture Agreement (No. 01-CR-11272166–060) with collaboration with the Forest Fire Laboratory, Pacific Southwest Research Station, USDA Forest Service, Riverside, CA, and the Forest Fire Laboratory, Rocky Mountain Research Station, USDA Forest Service, Missoula, MT. Special thanks to Joey Chong from the Riverside Forest Fire Laboratory, who helped with the collection of chaparral samples.

References

Albini FA (1976) Estimating wildfire behavior and effects. USDA Forest Service, Intermountain Forest and Range Experiment Station, General Technical Report GTR-INT-30. (Ogden, UT)

Andrews PL (1986) BEHAVE: fire behavior prediction and fuel modeling system–BURN subsystem, Part 1. USDA Forest Service, Intermountain Research Station, INT-194. (Ogden, UT)

Butler BW, Cohen J, Latham DJ, Schuette RD, Sopko P, Shannon KS, Jimenez D, Bradshaw LS (2004*a*) Measurements of radiant emissive power and temperatures in crown fires. *Canadian Journal of Forest Research* **34**, 1577–1587. doi:10.1139/X04-060

Butler BW, Finney MA, Andrews PL, Albini FA (2004*b*) A radiation-driven model for crown fire spread. *Canadian Journal of Forest Research* **34**, 1588–1599. doi:10.1139/X04-074

Byram GM (1959) Chapter 3: Combustion of forest fuels. In 'Forest Fire: Control and Use'. (Ed. KP Davis) pp. 61–89. (Maple Press Company: York, PA)

Catchpole WR, Catchpole EA, Tate AG, Butler BW, Rothermel RC (2002) 'A Model for the Steady Spread of Fire through a Homogeneous Fuel Bed.' (Millpress: Rotterdam)

Coleman JR, Sullivan AL (1996) A real-time computer application for the prediction of fire spread across the Australian landscape. *Simulation* **67**, 230–240. doi:10.1177/003754979606700402

Deeming JE, Lancaster JW, Fosberg MA, Furman RW, Schroeder MJ (1972) National Fire-Danger Rating System. RM-84. (Fort Collins, CO)

Dimitrakopoulos AP, Papaioannou KK (2001) Flammability assessment of Mediterranean forest fuels. *Fire Technology* **37**, 143–152. doi:10.1023/A:1011641601076

Engstrom JD, Butler JK, Smith SG, Baxter LL, Fletcher TH, Weise DR (2004) Ignition behavior of live California chaparral leaves. *Combustion Science and Technology* **176**, 1577–1591. doi:10.1080/00102200490474278

Forestry Canada Fire Danger Group (1992) Development and structure of the Canadian Forest Fire Behavior Prediction System. Forestry Canada Information Report ST-X 3. (Ottawa, ON)

Finney MA (1998) FARSITE: fire area simulator – model development and evaluation. USDA Forest Service, RMRS-RP-4.

Fletcher TH, Pickett BM, Smith SG, Spittle GS, Woodhouse MM, Haake E, Weise DR (2007) Effects of moisture on ignition behavior of moist California chaparral and Utah leaves. *Combustion Science and Technology* **179**, 1183–1203. doi:10.1080/00102200601015574

Fosberg MA, Deeming JE (1971) Derivation of the 1- and 10-hour timelag fuel moisture calculations for fire danger rating. USDA Forest Service, Rocky Mountain Forest and Range Experiment Station, Research Note RM-207. (Fort Collins, CO)

Lu H (2006) Experimental and modeling investigations of biomass particle combustion. PhD thesis, Brigham Young University, Provo, UT.

Pagni PJ, Woycheese JP (2000) Fire spread by brand spotting. In 'Proceedings: Fifteenth Meeting of the UJNR Panel on Fire Research and Safety. March 1–7, 2000. Volume 2'. (Ed. SL Bryner) National Institute of Standards and Technology, Information Report NISTIR 6588, pp. 373–380. (Gaithersburg, MD) Available at http://fire.nist.gov/bfrlpubs/fire00/PDF/f00131.pdf [Verified 30 September 2009]

Pickett BM (2008) Effects of moisture on combustion of live wildland forest fuels. PhD thesis, Brigham Young University, Provo, UT.

Rothermel RC (1972) A mathematical model for predicting fire spread in wildland fuels. USDA Forest Service, Intermountain Forest and Range Experiment Station, Research Paper INT-115. (Ogden, UT)

Smith SG (2005) Effects of moisture on combustion characteristics of live California chaparral and Utah foliage. MSc thesis, Brigham Young University, Provo, UT.

Tarifa CS, del Notario PP, Moreno FG (1965) On the flight paths and lifetimes of burning particles of wood. In '10th Symposium (International) on Combustion', 1964, Cambridge, UK. pp. 1021–1037. (The Combustion Institute: Pittsburgh, PA)

Van Wagner CE (1973) Height of crown scorch in forest fires. *Canadian Journal of Forest Research* **3**, 373–378. doi:10.1139/X73-055

Weise DR, White RH, Beall FC, Etlinger M (2005) Use of the cone calorimeter to detect seasonal differences in selected combustion characteristics of ornamental vegetation. *International Journal of Wildland Fire* **14**, 321–338. doi:10.1071/WF04035

Manuscript received 12 August 2008, accepted 22 December 2008